Sustainable Food Technology

ROYAL SOCIETY OF CHEMISTRY

PAPER

View Article Online
View Journal | View Issue

Check for updates

Cite this: *Sustainable Food Technol.*, 2025, **3**, 1164

Coconut oleosomes as a sustainable ingredient for food emulsion systems†

A. A. Anoop,[ab] P. M. Ramees[a] and K. V. Ragavan *[ab]

Virgin coconut meal (VCM), a major by-product from the coconut milk processing stream, contains 30–40% oil, which seldom gets repurposed for food applications. In this study, we investigated the feasibility of VCM for the extraction of oleosomes and its suitability for the formulation of emulsion-based food systems such as vegan mayonnaise. Oleosome extraction parameters (pH 6.43 and feed-to-solvent ratio 1 : 1.96) were optimised using the response surface methodology. The extracted oleosomes contain 93.24 ± 1.53% of fat and 5.34 ± 0.3% of proteins, along with residual carbohydrates and moisture. Particle and morphological analyses indicated that oleosomes are monodisperse spherical particles with a mean diameter of 1.35 μm, and they are highly stable in the pH range of 6–9. The functional and thermal properties of oleosomes were interpreted through FTIR and DSC analysis. The colour profile of oleosomes is neutral with excellent whiteness, making them suitable for the formulation of food products. Rheological analysis of oleosome incorporated mayonnaise exhibited a uniform structured biphasic food matrix with soft solid-like consistency on par with commercial mayonnaise. Sensory analysis using a nine-point hedonic scale revealed that oleosome-based mayonnaise is more appealing than egg-based mayonnaise. Results from the above studies suggest that VCM is a suitable by-product for the extraction of oleosomes, and the extracted oleosomes can act as an emulsion with the potential to replace oil and emulsifiers in emulsion-based food products. The above process can be effectively applied for the extraction of oleosomes from cold-pressed meals/seed cakes.

Received 26th March 2025
Accepted 20th May 2025

DOI: 10.1039/d5fb00112a

rsc.li/susfoodtech

Open Access Article. Published on 30 May 2025. Downloaded on 5/21/2026 5:07:34 PM.
This article is licensed under a Creative Commons Attribution-NonCommercial 3.0 Unported Licence.

Sustainability spotlight

Virgin coconut meal (VCM), a by-product from the coconut industry, is currently sold as animal feed or discarded in landfills and presents significant potential for repurposing. VCM has approximately 30% residual oil in the form of oleosomes. Leveraging these oleosomes for food applications could provide a sustainable solution, transforming VCM into a value-added ingredient. In this study, we have evaluated their potential for use as emulsifiers as well as a lipid source in the formulation of emulsion-based food products. Results from the experiments were encouraging and oleosomes exhibited excellent emulsification capacity for the production of clean label, sustainable plant-based mayonnaise. The study also highlights the possibility of valorization & sustainable processing of a coconut industry byproduct into a value-added ingredient for food formulations.

1 Introduction

Human food production systems significantly contribute to anthropogenic CO_2 emissions, accounting for approximately 26% of the total emissions. A major portion of these emissions arises from food loss, waste, and inefficient by-product utilization.[1] To mitigate this issue, the United Nations promotes the adoption of Sustainable Development Goals (SDGs) aimed at reducing emissions from food systems.[2] One effective approach is to repurpose food industry by-products into valuable ingredients using alternative and low-carbon footprint processes. Coconuts are an important food crop, with an annual global production of approximately 66.67 billion nuts in 2021.[3] A wide range of food products, including coconut oil, copra, desiccated coconut, coconut water, and coconut milk, are derived from coconuts.[4] The coconut industry also generates a number of by-products that often end up as feed or remain underutilized, leading to environmental disposal challenges and contributing significantly to greenhouse gas emissions.[5] It highlights the need for strategies that enhance the value of by-products from coconut processing.

Among these by-products, virgin coconut meal (VCM), a low-value product from the coconut industry, presents significant potential for repurposing. VCM is currently sold as animal feed at a mere 1.08–1.63 ₹ per kg (1.3–1.9 cents per kg) or discarded in landfills.[6] VCM is composed of 31.81% oil, 62.07% carbohydrates, and 5.19% protein.[7] Due to its favourable nutritional composition, several studies have evaluated the incorporation of VCM into bread, cookies, cakes, and noodles, however, the

[a]*CSIR-National Institute for Interdisciplinary Science and Technology, Thiruvananthapuram – 695019, India. E-mail: kvragavan@niist.res.in*

[b]*Academy of Scientific and Innovative Research (AcSIR), Ghaziabad-201002, India*

† Electronic supplementary information (ESI) available. See DOI: https://doi.org/10.1039/d5fb00112a

© 2025 The Author(s). Published by the Royal Society of Chemistry

Open Access Article. Published on 30 May 2025. Downloaded on 5/21/2026 5:07:34 PM. This article is licensed under a Creative Commons Attribution-NonCommercial 3.0 Unported Licence.

commercial application remains limited.[8–11] Most research focuses primarily on extracting protein from VCM,[7,12,13] often neglecting the residual 30% oil, which is stored as oleosomes. These organelles are naturally occurring vesicles in plant cells that encapsulate lipids, serving as energy reservoirs in seeds/nuts.[14] Oleosomes predominantly contain triacylglycerol (TAG), constituting about 92% of the dry matter, with about 7% protein covering the TAG core, and less than 1% phospholipids.[15] Leveraging these oleosomes for food applications could provide a sustainable solution, transforming VCM into a value-added ingredient.

Oleosomes are extracted from soybeans, rapeseed, and sunflower seeds for food application.[16–20] However, to our current understanding, limited research has been conducted on extracting oleosomes from coconut industry by-products, particularly from VCM, and evaluating their potential for food applications. Aqueous extraction is commonly employed for extracting oleosomes, where the raw material is soaked in water and blended to disrupt the cell wall to effectively release the intracellular components into the aqueous medium. Oleosome extraction is further improved by pre-treatment techniques such as enzyme, ultrasound, and twin screw pressing/extrusion.[14,21–23] Oleosomes are increasingly used as a healthy fat substitute for the formulation of dairy alternatives, yoghurt, sauces, salad dressings, mayonnaise, ice creams, chocolate, and edible films.[17,24–28] The primary objective of this research work is to develop a green and scalable method for the extraction of oleosomes from VCM and optimize the extraction parameters to achieve maximum yield. Characterize the extracted oleosomes to ascertain their physicochemical and functional properties to assess their suitability in the formulation of plant-based emulsion foods.

2 Materials and methods

2.1 Raw material & chemicals

VCM, a by-product obtained after the extraction of coconut milk, was used as the raw material for oleosome extraction. The VCM was received as a gift from Apex Coco and Solar Energy Limited, Tamil Nadu, India. Nile Red and Fluorescein isothiocyanate (FITC) were purchased from TCI, Japan. Analytical grade HCl, NaOH, and hexane were purchased from Sigma-Aldrich, USA. Vinegar, salt, sugar, coconut oil, remaining ingredients were procured from the regional market. All experiments were conducted using double-distilled water.

2.2 Oleosome extraction

The VCM was soaked with double-distilled water in a 1 : 10 ratio and then blended using a commercial blender with a power rating of 1300 W at about 6000 rpm for 4 min. The resulting slurry was strained across a double-layered cheesecloth, and the filtrate was collected and centrifuged at 10 000 rpm for 20 min at 25 °C. The oleosome-rich top layer was dispersed in distilled water (1 : 5 ratio) and subjected to an additional centrifugation step under the same conditions. The top layer was collected as the purified oleosome fraction for subsequent analysis and product formulation. Yield was calculated using eqn (1).

$$\text{Yield}(\%) = \left(\frac{\text{Weight of extracted oleosome(g)}}{\text{Weight of initial VCM(g)}}\right) \times 100 \quad (1)$$

2.3 Optimization of the oleosome extraction

To optimize the extraction parameters, Response Surface Methodology (RSM) was applied. The experimental design was constructed using Design-Expert 13 software, implementing a Box–Behnken design.[29] Three independent variables of the extraction process, such as pH (4, 7, 10), soaking time (0, 12, 24 h), and solvent ratio (1 : 5, 1 : 10, 1 : 15) were considered with yield as the dependent variable. A total of 17 experimental runs were conducted, including five replicates at the center point to assess experimental variability. For the extraction process, VCM was soaked in double distilled water according to the predetermined durations and ratios identified in the RSM design. The pH of each soaked sample was adjusted to the predetermined levels using 0.1 M HCl or 0.1 M NaOH. Following pH adjustment, the oleosomes were extracted and purified using the process described in Section 2.2. The purified oleosome fraction was collected for subsequent analysis and product formulation.

2.4 Proximate analysis of oleosome

Extracted oleosomes were dried using a freeze dryer (VirTis SP Scientific Wizard 2.0, USA), and their proximate composition was analysed in triplicate.[30]

2.4.1 Determination of moisture content. The residual moisture present in the sample was analysed according to the AOAC method 934.01 (AOAC, 2000). Approximately 2–3 g of samples are weighed and kept in pre-weighed, clean glass Petri dishes. These samples were then dried in a hot air oven (Binder, ED 115, France) at 105 °C for 3 h or until a constant weight was achieved. The moisture content was calculated based on the weight difference before and after drying the samples.

2.4.2 Determination of oil content. The oil content was analysed using the Soxhlet extraction method, AOAC 954.02 (AOAC, 2000). Typically, 5 g of sample was placed in a thimble and refluxed using *n*-hexane for 6 h for complete recovery of oil from the sample.

2.4.3 Determination of protein content. The protein content was analysed using the AOAC 2001.11 by the micro Kjeldahl method (Kjeltec™ 8400, Denmark). The nitrogen content was determined and converted to protein using a standard conversion factor of 6.25.

2.4.4 Determination of ash content. The ash content of the oleosomes was analysed according to AOAC method 942.05 (AOAC, 2000). The sample was weighed and transferred to a porcelain crucible, which was then placed in a muffle furnace and incinerated at 550 °C for 6 h until a light grey or white ash was obtained. The crucible containing the ash was cooled and weighed to calculate the ash content.

2.5 Preparation of vegan mayonnaise

The vegan mayonnaise was prepared using oleosome as the base ingredient, comprising 94.05% of the total formulation. To this,

Open Access Article. Published on 30 May 2025. Downloaded on 5/21/2026 5:07:34 PM. This article is licensed under a Creative Commons Attribution-NonCommercial 3.0 Unported Licence.

4.38% vinegar (v/w relative to oleosome) was added using a pipette. Salt and sugar were then added at 1% and 0.66% (w/w relative to oleosome), respectively. All ingredients were combined in a mixing bowl and thoroughly blended using a domestic blender. The mixing process continued until a homogeneous, creamy consistency was achieved, indicative of a stable emulsion. For the control mayonnaise, 40 g of egg was combined with 100 mL of coconut oil, forming the base. Similar portions of vinegar, salt, and sugar relative to the base ingredients were added to maintain consistency between formulations. Coconut oil was used in the control to provide a valid comparison, as the oleosome-based mayonnaise is essentially composed of encapsulated coconut oil.

2.6 Particle size determination

The droplet size of the extracted oleosomes was determined using a Malvern Zetasizer (Zeta Nano-ZS; Malvern Instruments, UK), which relies on the dynamic light scattering (DLS) principle. 20 mg of the sample was diluted with 75 mL of 0.1% sodium dodecyl sulfate (SDS) solution and gently stirred with a spatula until fully dispersed, and the particle size was measured at room temperature with 10 cycles. The refractive indices used for the calculations were 1.46 for oleosomes and 1.33 for the distilled water.[31]

2.7 Zeta potential analysis

The zeta potential of the oleosomes was measured over a pH range of 2 to 10 using the Malvern Zetasizer (Nano ZS; Malvern Instruments, UK). Oleosomes were diluted with distilled water in a ratio of 1 : 100 (100 μL of oleosome dispersion in 10 mL of distilled water), and the pH was adjusted using 0.1 M HCl and 0.1 M NaOH. Measurements were conducted on three independent samples, and the average zeta potential was recorded for each pH.

2.8 Fourier transform infrared spectroscopy

FTIR spectra were obtained for VCM, coconut milk, oleosome, and residue using an ATR-FTIR spectrophotometer (Bruker Alpha-T, Germany). A diamond ATR crystal was used, and it was cleaned with isopropanol after each measurement. The background spectrum was recorded over a wavenumber ranging from 400–4000 cm^{-1} with a resolution of 4 cm^{-1}. The background was scanned 32 times, and the average of these scans was used as the background spectrum.

2.9 Differential scanning calorimetry

Precisely weighed samples of 3–5 mg were taken in 40 μL aluminium DSC pans and hermetically sealed. The sample pans were analyzed using a TA Instruments DSC Q2000 along with a hermetically sealed empty DSC pan as reference under a nitrogen flow of 50 mL min^{-1}, with a heating rate of 10 °C min^{-1}, spanning from −20 °C to 120 °C. Data were processed using the Universal Analysis software from TA Instruments.

2.10 Fluorescence microscopy

The morphology of the oleosome fractions and the distribution of oil and protein in the oleosome were analyzed using a fluorescence microscope (IX83 inverted microscope, Olympus Life Science). The oleosome samples were diluted with double-distilled water in a ratio of 1 : 9 (w/w) and stirred for 30 min. Lipids in the resulting solution were stained with 5 μL of 0.1% (w/v) Nile red solution with excitation and emission at 488 nm and 500–600 nm, respectively. Proteins were stained with 10 μL of 0.1% of (w/v) FITC (fluorescein isothiocyanate) solution with excitation and emission at 633 nm and 650–750 nm, respectively. Relative fluorescence intensity of Nile red to FITC was calculated using ImageJ software.

2.11 Colour analysis

The colour profile of oleosome and mayonnaise samples was measured using a Hunter Lab Colorimeter (ColorFlex EZ, Virginia, USA) to determine the CIE L^*, a^*, and b^* values. The reference calibration plate had standard L^*, a^*, and b^* values of 98.014, −0.032, and 1.459, respectively. All readings were recorded in triplicate. The total colour difference (ΔE) of samples was calculated using eqn (2) as described below.[32]

$$\Delta E = \sqrt{\left(L_{\text{sample}} - L_{\text{standard}^*}\right)^2 + \left(A_{\text{sample}} - A_{\text{standard}^*}\right)^2 + \left(B_{\text{sample}} - B_{\text{standard}^*}\right)^2} \quad (2)$$

2.12 Rheology

Rheological properties of mayonnaise samples were analyzed using an Anton Paar Modular Compact Rheometer MCR102 (Anton Paar GmbH, Graz, Austria) equipped with a CP25-2 measuring system (25 mm diameter, 2° cone angle) and a fixed gap of 0.1 mm. Temperature was controlled at 25 ± 0.1 °C using a Peltier temperature control system. Oscillatory tests were performed using the RHEOPLUS/32 V3.62 software. An amplitude sweep test was conducted by increasing the strain (γ) logarithmically from 0.01% to 100% at a fixed angular frequency (ω) of 5 rad s^{-1} to determine the linear viscoelastic region (LVR).

2.13 Texture analysis

The textural characteristics of the oleosome samples were assessed using a TA.XT Plus texture analyser (Stable micro systems, UK), using a cylindrical probe of 25 mm diameter and a 25 kg load cell. Prior to analysis, the samples were equilibrated at room temperature (25 ± 1 °C). A consistent speed of 1 mm s^{-1} was maintained during pre-test, test, and post-test, with a penetration distance of 3 mm and a contact time of 3 s.

© 2025 The Author(s). Published by the Royal Society of Chemistry

Open Access Article. Published on 30 May 2025. Downloaded on 5/21/2026 5:07:34 PM. This article is licensed under a Creative Commons Attribution-NonCommercial 3.0 Unported Licence.

2.14 Sensory analysis

Sensory analysis of the mayonnaise samples were conducted with 20 semi-trained panelists in a dedicated sensory laboratory. Mayonnaise samples were served alongside freshly prepared plain potato chips. Panelists assessed ten sensory attributes of the product including appearance, colour, texture, taste, flavour, aroma, mouthfeel, creaminess, consistency, and overall acceptance, using a nine-point hedonic scale (1 = "dislike extremely", 9 = "extremely likely"). Samples were assigned random codes and presented in a randomized order.

3 Result and discussion

3.1 Proximate analysis

Proximate composition of freeze-dried VCM oleosomes contains 93.24% ± 1.53% fat, with smaller amounts of protein (5.34% ± 0.3%), carbohydrate (0.89%), moisture (0.42% ± 0.1%), and ash (0.11% ± 0.05%) (Table 1). These results are in agreement with the reported studies on oleosomes extracted from oilseeds.[33] The exceptionally high fat content aligns with the oleosomes' role as lipid storage organelles in plant cells, indicating an effective extraction process. The presence of protein, though relatively low, likely corresponds to the structural proteins mainly oleosin, caleosin, and steroleosin, which form the outer membrane of the oleosomes, essential for their stability.[34] The freeze-drying process minimises moisture, which helps inhibit lipid oxidation and improves shelf life. Notably, previous studies have shown that oleosome-encapsulated oils exhibit enhanced oxidative stability compared to emulsions stabilised with surfactants such as SDS or Tween 20.[35] This intrinsic structural protection is likely applicable to coconut oleosomes as well, which will help in preserving lipid quality during storage, making them stable lipid carriers in food formulations.

3.2 Response surface methodology

The RSM analysis identified the optimal extraction condition for obtaining maximum yield at pH 6.43 and a VCM to distilled water ratio of 1 : 9.96 (Fig. 1). Soaking time was found to have an insignificant impact on oleosome extraction due to the prior wet processing in coconut milk extraction, which removes most of the water-soluble components. Additionally, the wet grinding step in our extraction process likely minimized the need for prolonged soaking. Oleosomes exhibited a ζ-potential of −18.13 mV at pH 6 which further decreased to −24.53 mV at pH 7. A pH of 6.43 resulted in maximum yield of oleosomes from VCM. The higher negative surface charge at this pH enhanced electrostatic repulsion between oleosomes, facilitating their separation and improving purity.[36] On the contrary, VCM oleosomes exhibited neutral surface charge between pH 5 and 6, and at this point, electrostatic or hydrophobic interactions between the oleosome interface and co-extracted proteins likely contributed to lower yields.[23,37] The solvent ratio demonstrated moderate influence on extraction efficiency with optimal performance observed at a 1 : 9.96 VCM to distilled water ratio. Lower ratios reduced extraction effectiveness, whereas higher ratios were avoided due to their negative impact on techno-economic feasibility. The model showed a determination coefficient (R^2) value of 83.36%, indicating a good fit between the observed and predicted data. Furthermore, the Adequate Precision value of 5.24 exceeds the desirable threshold of 4.0, signifying a sufficient signal-to-noise ratio for navigating the design space. Overall, the model supports the extraction parameters with acceptable accuracy for potential scale-up.

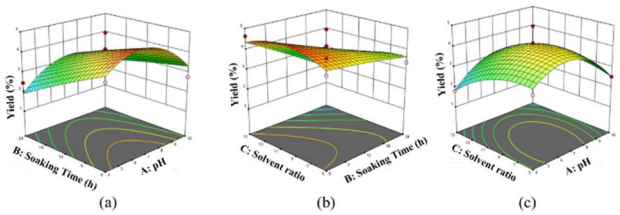

Fig. 1 Three-dimensional response surface graphics depicting the influence of independent factors on oleosome yield. (a) Interaction between soaking time and pH; (b) interaction between solvent ratio and soaking time; (c) interaction between solvent ratio and pH.

Table 1 Proximate composition of VCM and oleosome[a]

	VCM	Oleosome
Residual moisture (%)	6.41 ± 0.14[a]	0.42 ± 0.10[b]
Ash (%)	3.38 ± 0.16[a]	0.11 ± 0.05[b]
Protein (%)	17.38 ± 0.49[a]	5.34 ± 0.30[b]
Fat (%)	39.05 ± 1.68[b]	93.24 ± 1.53[a]
Carbohydrate (%)	33.78[a]	0.89[b]

[a] Values are reported as mean ± standard deviation. Superscript letters (a and b) in each row indicate statistically significant differences between means ($p < 0.05$), as determined by Tukey's *post hoc* test.

3.3 Droplet size determination

Particle/droplet size of ingredients impacts the product's rheology, stability, and mouthfeel. Smaller, uniform droplets ensure a smoother consistency and help prevent phase separation, resulting in a stable emulsion. The average droplet size of VCM oleosomes was found to be 1.35 ± 0.1 μm with a unimodal size distribution around 0.47 μm indicating a stable and uniform oleosome particles (Fig. S1a†). Oleosomes from oilseeds are reported to have similar sizes, typically below 2 μm.[38–41] In some of the studies, oleosomes with larger droplet sizes are reported to be unstable, which might be due to flocculation, coalescence, or due to the presence of extraneous materials.[23,40] In contrast, the smaller droplet size in this study indicates higher purity and successful preservation of the native structure of the extracted oleosomes.[38]

The droplet size of both VCM oleosome mayonnaise (1.52 ± 0.11 μm) and control mayonnaise (1.16 ± 0.06 μm) is relatively close, suggesting that both formulations should exhibit similar textural properties, such as creaming and mouthfeel. In both the control and VCM based mayonnaise, bimodal distribution was observed instead of unimodal distribution (Fig. S1b & c†).

Open Access Article. Published on 30 May 2025. Downloaded on 5/21/2026 5:07:34 PM. This article is licensed under a Creative Commons Attribution-NonCommercial 3.0 Unported Licence.

The slight difference in particle size is unlikely to affect these sensory attributes, as emulsions with particle sizes in this range generally produce a smooth and creamy texture.[17] It is important to note that the above particle size is achieved without emulsifier or high energy dispersion technique such as homogenisation or sonication whereas in commercial mayonnaise emulsifiers are added and homogenised to achieve the droplet size. In the case of VCM oleosome mayonnaise, the oleosomes naturally stabilize the emulsion due to their unique protein–phospholipid shell layer, which mimics the emulsifying function of egg proteins in the control mayonnaise. Despite the different stabilizing mechanisms, both types of emulsions demonstrated a comparable creamy mouthfeel as evidenced by sensory analysis. VCM oleosome-based mayonnaise scored 7.85 for creaminess on a nine-point hedonic scale, slightly outperforming egg-based mayonnaise, which scored 7.35. This indicates that VCM oleosome mayonnaise can successfully replicate the sensory attributes of traditional mayonnaise, establishing it as a promising plant-based alternative. Detailed sensory evaluation of the products is discussed in Section 3.11.

3.4 Zeta potential

Zeta potential, or electrokinetic potential, is the electric potential on the interface of colloid particles as they move through an electric field.[42] It is a key indicator of the stability of oleosomes in dispersions, with higher absolute zeta potential values indicating stronger electrostatic repulsion, leading to more stable emulsions.[43] The stability and flocculation behaviour of oleosome suspensions are influenced by electrostatic interactions between the associated proteins. Among these proteins, Oleosin is the major protein that forms a layer over the lipid core and interacts with the ions distributed around them, forming what's known as an electrical double layer.[14,42] Oleosins have charged N and C terminals, with positive charges facing inward and negative charges exposed to the external environment.[44] The zeta potential of oleosomes was +25.6 ± 0.21 mV at pH 2.0 and −46.8 ± 0.33 mV at pH 11.0, with an isoelectric point observed around pH 5.0 (Fig. 2). These results are in agreement with previous studies on soybean oleosome where zeta potential values ranged from +15 mV at pH 2.0 to −26.5 mV at pH 9.0, exhibiting an isoelectric point of pH 5.0.[45] At lower pH, proteins associated with the oleosome surface undergo protonation, resulting in a positive surface charge, while at higher pH, deprotonation induces a negative charge.[46] As the pH deviated from the isoelectric point, the absolute zeta potential values increased, reflecting enhanced stability due to stronger electrostatic repulsion. The variation in pH affects not only the net surface charge of the oleosomes but also the exposure of hydrophilic regions and the tertiary confirmation of the oleosome-associated proteins. These alterations, consequently, affect their charge-binding ability and the distribution of surface charge.[47] These findings underscore the importance of pH controlling in maintaining stable oleosome suspensions, particularly for food applications.

3.5 FTIR

The FTIR analysis revealed the lipid-rich nature of the oleosome fraction obtained from VCM (Fig. 3). The sharp and narrow peak at 2921 cm^{-1} is attributed to CH and CH_2 which represent the asymmetric stretching vibrations of the aliphatic methylene group (Table 2). Additionally, the narrow peak at 2854 cm^{-1} belongs to the symmetric stretching vibrations of the aliphatic methylene group. Both these peaks are commonly found in the fatty acid chains of oils and fats.[48,49] The peak observed at 1745 cm^{-1} is indicative of the stretching vibration of the carbonyl ester (C═O) group associated with triglycerides present in coconut meat. Previous research has commonly identified this peak as a characteristic marker for fatty molecules in biological systems, representing plant oils and animal fats.[49,50] The peak observed at 1463 cm^{-1} is attributed to the bending vibrations of aliphatic hydrocarbons, specifically the

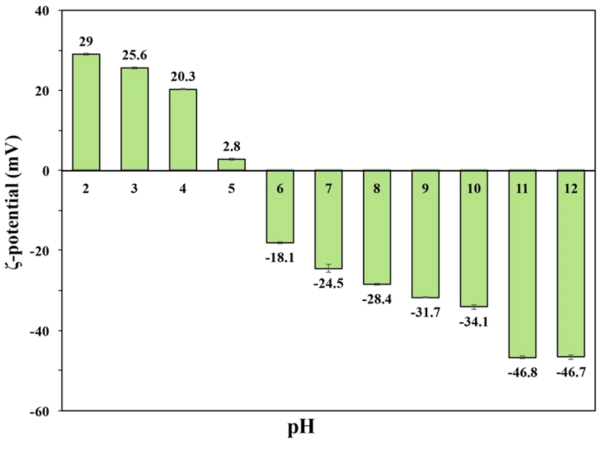

Fig. 2 Zeta potential (mV) of the oleosomes across a pH range of 2 to 12, with an isoelectric pH observed between pH 5 and 6. Oleosomes were found to be stable in the pH range 7–9 with zeta potential values above −25 mV.

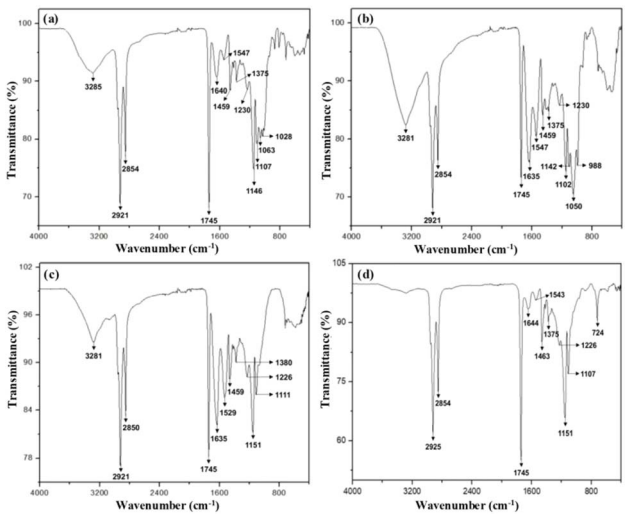

Fig. 3 FTIR spectra of different fractions of (a) VCM; (b) lyophilized coconut milk; (c) coconut pellet and (d) lyophilized oleosome.

© 2025 The Author(s). Published by the Royal Society of Chemistry

Open Access Article. Published on 30 May 2025. Downloaded on 5/21/2026 5:07:34 PM. This article is licensed under a Creative Commons Attribution-NonCommercial 3.0 Unported Licence.

CH_2 and CH_3 groups, which are commonly present in the hydrocarbon chains of fatty acids and lipids.[51] The band observed at 724 cm^{-1} is likely due to the combined effects of CH_2 rocking vibration and the out-of-plane deformation of *cis*-disubstituted olefins. The presence of this vibration mode suggests the existence of *cis* double bonds (C=C) with two substituents on the same side of the double bond. This is commonly found in unsaturated fatty acids, such as oleic acid (*cis*-9-octadecenoic acid), a major component of coconut oil.[48,49] Overall, these spectral features are consistent with the previous reports on coconut oleosomes, further validating the composition of the extracted fraction.[52]

Additionally, the peak observed at 1375 cm^{-1} corresponds to C–H bending vibrations of alkane CH_3 groups and the peaks at 1102/1151 cm^{-1} represent the stretching vibrations of the C–O bond in ester groups, further confirming the presence of various hydrocarbon chains, alkyl groups, and ester functional groups, respectively, indicative of fatty acids, lipids, and triglycerides.[53,54] These peaks are present in the VCM and in all three fractions (coconut milk, pellet, and oleosomes) with varying intensities, with the oleosome fraction showing the highest intensity. The presence of these bands in the oleosome fraction is correlated to its high oil content. The occurrence of these bands in the coconut milk fraction might be due to the presence of free oil. Furthermore, the presence of these bands in the residual fraction indicates the presence of intact oleosomes in the flour, even after the extraction process.

A peak around 1635 cm^{-1} in the FTIR spectra of all fractions can be attributed to the amide I region, which arises from the C=O stretching of the peptide bonds (–CO–NH–) present in proteins. The amide I band, usually observed within the 1600–1700 cm^{-1} range, serves as a characteristic marker for the presence of proteins or peptides in a sample. The observation of this peak in the coconut milk fraction (Fig. 3b) can be explained by the presence of albumins (20% of total coconut protein), which are water-soluble proteins found in coconut meat and gets extracted into the coconut milk during the extraction process.[55] The intensity of this peak is highest in the coconut residue fraction, indicating a higher protein content in the pellet compared to the other fractions. In the oleosome fraction, the intensity of the peak is very low, which correlates with the expected low protein content of oleosomes, as they are primarily composed of oil. The peak observed around 1547 cm^{-1} in the FTIR spectra of VCM and coconut milk can be assigned to the amide II band, which is linked to the α-helix structure of proteins. This band primarily originates from the N–H bending vibrations (40–60%) and secondarily from the C–N stretching vibrations (18–40%) of the peptide bonds.[56,57] The presence of this peak in VCM and coconut milk indicates the presence of proteins containing α-helical structures in their secondary conformation. The higher intensity of this peak in the coconut milk fraction suggests that a significant portion of proteins containing α-helical structures were extracted into the coconut milk. In the case of oleosome fraction, the reduced intensity and slight shift of the peak to 1543 cm^{-1} can be attributed to the lower overall protein content in the oleosomes, as they are predominantly composed of oil bodies. However, the presence of this peak indicates that some proteins, including those with α-helical structures, were carried over into the oleosome fraction during extraction. In contrast, the coconut pellet fraction exhibits a high intensity of the peak, but it is shifted to 1529 cm^{-1}. This shift in wavenumber could be due to changes in the protein conformation or interactions within the pellet matrix, which can affect the vibrational frequencies of the peptide bonds. The high intensity of the peak in the pellet fraction suggests that a significant portion of the α-helix-containing proteins remained in the solid residue after the extraction process, mainly the water-insoluble coconut protein fractions, in particular globulin, glutelin-1, glutelin-2 and prolamines.[55] The variations in peak intensity and position among the different fractions can be attributed to the partitioning of proteins during the extraction process, as well as potential changes in their conformations or interactions within the respective matrices. A peak was observed at 1230 cm^{-1} in the FTIR spectra of all samples, representing the amide III band, which results from the coupled vibrations of C–N stretching and N–H bending in the peptide bonds present in proteins and peptides.[58] The presence of this peak in all samples indicates the presence of proteins or peptides in all fractions, albeit in varying amounts.

The bands observed in the 980–1050 cm^{-1} range in coconut milk and VCM are associated with C–O stretching vibrations in polysaccharides, indicating the presence of carbohydrates.[59] These peaks are likely attributed to water-soluble carbohydrates, which are absent in the oleosome and pellet (insoluble residue) fractions. Coconut milk and VCM contain various water-soluble carbohydrates, such as sugars and soluble dietary fibers, which could contribute to the observed peaks in the

Table 2 FTIR absorption band for the corresponding vibration types and functional groups

Wavenumber (cm^{-1})	Functional group	Vibration type	Assignment	Reference
3280–3285	O–H	Stretching	Polysaccharides	56 and 60
2920–2925	CH, CH_2	Asymmetric stretching	Lipid chain	48 and 49
2850–2855	CH_2	Symmetric stretching	Lipid chain	48 and 49
1745	C=O	Stretching	Triglycerides	49 and 50
1635–1645	C=O	Stretching	Protein	55
1540–1550	N–H/C–N	Bending/stretching	Protein	56 and 57
1220–1230	N–H/C–N	Bending/stretching	Protein	58
980–1050	C–O	Stretching	Polysaccharides	59

© 2025 The Author(s). Published by the Royal Society of Chemistry

Open Access Article. Published on 30 May 2025. Downloaded on 5/21/2026 5:07:34 PM. This article is licensed under a Creative Commons Attribution-NonCommercial 3.0 Unported Licence.

specified wavenumber range. Additionally, the broad peak around 3400 cm^{-1} represents the O–H stretching vibrations of both D-glucose and D-fructose, which can be found in both soluble and insoluble carbohydrates.[56,60] The coconut milk fraction exhibited a broader peak in this range compared to the pellet, suggesting a higher concentration of polar compounds contributing to the stretching vibration of soluble sugars. Additionally, the absence of this peak in the oleosomes confirms the lack of carbohydrates in the oleosome fraction.

3.6 DSC analysis

The DSC of VCM exhibits a broad endothermic peak at 70.54 °C, characteristic second-order thermal transition, indicating it's amorphous nature (Fig. 4a). Unlike first-order transitions, where latent heat is involved, a second-order transition is marked by a gradual change in heat capacity without the release or absorption of latent heat. This gradual transition suggests a more disordered structure in the VCM, possibly due to the matrix composed of proteins, carbohydrates and lipids in a random arrangement. In literature, coconut meal is reported to have a T_d of 83 °C, whereas the VCM used in this study has a T_d of 70.5 °C which is attributed to the residual fat content.[61] This residual oil likely act as plasticizer due to its higher heat capacity thereby denaturing/unfolding proteins at lower temperature. In contrast, VCM oleosomes exhibit a sharp endothermic peak at 25.4 °C (Fig. 4b). It is a characteristic melting profile of coconut oil, which has a higher amount of medium-chain saturated fatty acids. Lauric acid (C12) comprises close to 47% of the total fatty acid content in coconut oil, followed by myristic acid (C14) and palmitic acid (C16) with 18 at and 8% respectively.[62,63] All these fats exhibit melting points below 35 °C, consistent with the observed DSC peak. The DSC thermogram has a straight line after 32.5 °C, indicating a constant heat flow, which suggests that the complete phase transition from solid fat to liquid has occurred, reflecting the melting of all fats contained in the oleosomes.

3.7 Fluorescence microscopy

The oleosomes appear as distinct spherical bodies varying in size from small punctate structures to larger globular entities in fluorescence microscope images (Fig. 5). Two different fluorescent dyes, Nile red and FITC, were used to simultaneously visualise the lipid and protein components of the oleosomes, respectively. Fig. 5a, represents the initial oleosome fraction with single centrifugation step, which has a significant amount of green fluorescence from the protein and the presence of non-oleosome components, such as surfactants or other impurities.[64] A significant portion of the non-oleosome impurities, have been removed with two rounds of centrifugation (Fig. 5b). The oleosomes appear more distinct and well-separated, also there is a noticeable reduction in the amount of diffuse green fluorescence (FITC-labeled proteins) compared to Fig. 5a. This correlates with the increasing red-to-green fluorescence ratio observed after each step of centrifugation. Fluorescence ratio increased from 0.54 a.u. after the first centrifugation to 0.57 a.u. and 0.62 a.u. after the second and third steps, respectively. This suggests that the purification step may have enriched the oleosome fraction for the protein components relative to the lipid components. Oleosomes with three rounds of centrifugation (Fig. 5c) depict the purest oleosome fraction. The green fluorescence signal appears to be predominantly associated with the distinct spherical oleosome structures themselves, with minimal diffuse background fluorescence. This observation indicates that the successive centrifugation steps resulted in a highly purified oleosome fraction devoid of non-oleosome components. It is critical for ingredients to have maximum purity to control the product characteristics in food formulation.

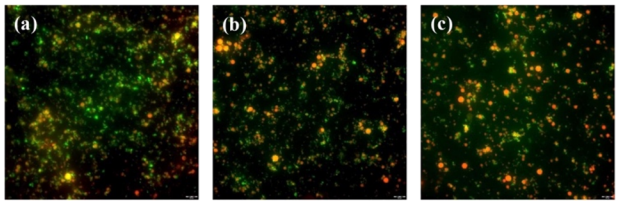

Fig. 5 Fluorescence microscopy images at 40× magnification of oleosome extract after (a) first centrifugation, (b) second centrifugation, (c) and third centrifugation. Proteins labelled with FITC appear green, while lipids stained with Nile red appear red.

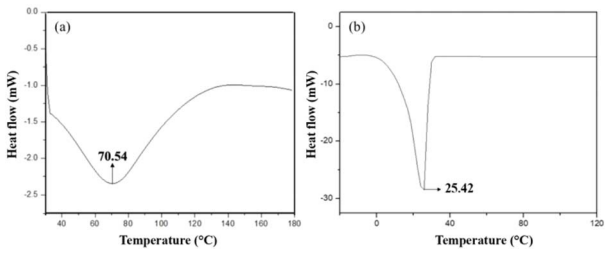

Fig. 4 DSC of (a) VCM and (b) VCM oleosomes. The DSC analysis for VCM was conducted over a temperature range of 30 °C to 180 °C, while that of VCM oleosomes was performed over a range of −20 °C to 120 °C to assess their melting profiles. A heating rate of 10 °C per minute was used in both cases.

3.8 Colour analysis

The colour profiles of VCM, VCM oleosome, and coconut oil extracted from the oleosomes were analyzed, followed by the colour recordings of oleosome-based and control mayonnaise in CIE format (L^* a^* b^*) (Fig. 6). VCM exhibited a high lightness value ($L^* = 90 \pm 0$) with a slight red hue ($a^* = 1 \pm 0$) and a pronounced yellow hue ($b^* = 15.32 \pm 0.01$). This light-coloured appearance with a noticeable yellow hue is likely due to natural pigments such as carotenoids or other phenolic compounds retained during the processing of VCM.[65] VCM oleosomes have almost similar lightness ($L^* = 89.68 \pm 0.02$) of VCM, however with a shift towards green ($a^* = -0.46. \pm 0$) and a reduced yellow hue ($b^* = 4.56 \pm 0.01$). Compared to the VCM, the yellow hue in the oleosomes could be attributed to the extraction process, which isolates lipid-rich oleosomes and

 © 2025 The Author(s). Published by the Royal Society of Chemistry

Open Access Article. Published on 30 May 2025. Downloaded on 5/21/2026 5:07:34 PM. This article is licensed under a Creative Commons Attribution-NonCommercial 3.0 Unported Licence.

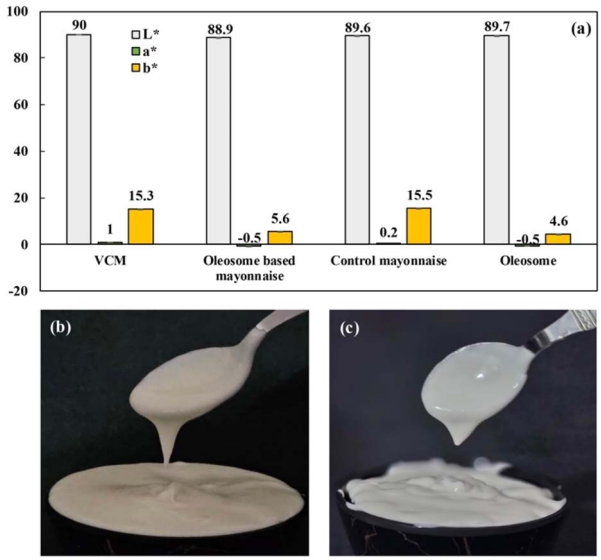

Fig. 6 (a) CIELAB colour parameters of VCM, oleosome-based mayonnaise, control mayonnaise and oleosomes. L^*, a^* and b^* values are represented in light grey, green and yellow bars respectively. Macro images of (b) control mayonnaise and (c) oleosome-based mayonnaise.

potentially reduces the concentration of pigments and other coloured compounds originally present in the VCM.

Coconut oil, extracted from these oleosomes, exhibited significantly reduced lightness ($L^* = 1.56 \pm 0.02$) and nearly neutral colours on both the red-green ($a^* = -0.01 \pm 0.03$) and yellow-blue ($b^* = -0.37 \pm 0.02$) axes. These values are consistent with previously reported studies.[66] The near absence of any significant hue in the oil suggests it is largely devoid of pigments.

The colour profile of control mayonnaise prepared using eggs and oleosome-based mayonnaise are compared. Lightness and greenness of the products are almost same, whereas the yellowness of the products varied to a great extent with control mayonnaise having b^* value of 15.54 ± 0.05 compared to 5.63 ± 0.04 of oleosome-based mayonnaise. The yellow color of control mayonnaise is derived from egg yolk, which is rich in carotenoid pigments.[67] The colour differences (ΔE) compared to the calibration standard were 16.41 ± 0.06 for control mayonnaise and 10.05 ± 0.04 for oleosome-based mayonnaise, indicating that the latter had a closer match to the neutral white standard. Sensory evaluation scores for colour were also higher for the oleosome-based sample (8.3) compared to the control (7.25), indicating better visual appeal and potential consumer preference. Additionally, the lower b^* value of the oleosome-based mayonnaise may enhance shelf-life stability, as reduced carotenoid content minimises the risk of oxidation and colour degradation during storage.[68] These results suggest that the oleosome-based formulation is better than the control mayonnaise.

3.9 Texture analysis

Texture analysis of oleosomes extracted from VCM revealed unique properties with potential applications in imitation milk and emulsion-based products. The oleosomes exhibited a slightly negative cohesiveness ($-7.75 \times 10^{-2} \pm 0.01$ N), indicating a tendency to disperse rather than aggregating. Oleosomes exhibit a relatively high consistency (3.58 ± 0.05 N mm) and moderate hardness ($5.01 \times 10^{-1} \pm 0.01$ N), suggests that they could contribute to stable emulsions with a creamy texture. The low index of viscosity ($7.2 \times 10^{-3} \pm 0$ N mm) further indicates good flow properties, which could be advantageous in formulating soft solid food products. These textural properties collectively suggest that VCM oleosomes have the potential to mimic the mouthfeel and stability of fat in plant-based alternatives, while also offering unique textural attributes that could lead to innovative food products.

3.10 Rheology

Rheology of emulsion-based foods provides key insights about their flow behaviour based on the relationship between storage (G') and loss (G'') moduli. All samples predominantly exhibit solid-like behaviour at low strains, with G' greater than G'' (Fig. 7). As the shear rate increases, their viscosity decreases, demonstrating typical pseudo plasticity observed in stable emulsions like mayonnaise.[69] The non-linear response of all samples (shear thinning) is consistent and further confirms their non-Newtonian nature.[70,71] Among the samples, the novel vegan mayonnaise made with VCM oleosome exhibited initial storage (G') and loss (G'')

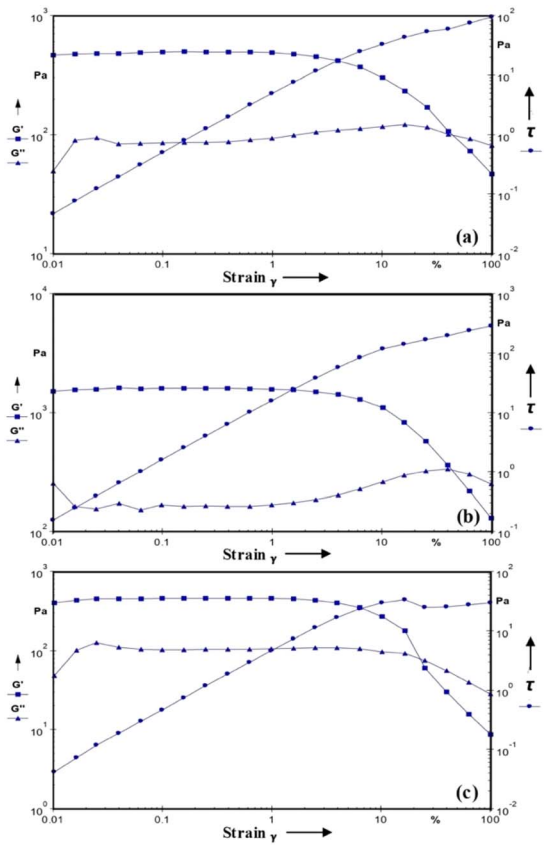

Fig. 7 Rheological profile of the (a) control mayonnaise (b) oleosome-based mayonnaise, and (c) commercial mayonnaise.

Open Access Article. Published on 30 May 2025. Downloaded on 5/21/2026 5:07:34 PM. This article is licensed under a Creative Commons Attribution-NonCommercial 3.0 Unported Licence.

moduli of approximately 400 Pa and 50 Pa, respectively. It maintained a stable linear viscoelastic region (LVR) up to about 10% strain, with a crossover point ($G' = G''$) occurring at around 25% strain. This indicates a softer solid-like character that gradually transitions to more liquid-like behaviour, suggesting a more easily spreadable texture that may break down more readily under stress and provide a quick melt-in-mouth sensation, characteristic of a softer, less rigid structure. In comparison to the oleosome-based sample, the control mayonnaise, made with coconut oil and egg as an emulsifier, exhibited higher initial moduli values, with G' around 490 Pa and G'' approximately 85 Pa. It maintained a stable LVR up to about 16% strain, with a crossover point observed at around 40% strain. This suggests a more robust structure that retains its solid-like behaviour at higher strain levels and resists flow more effectively than the oleosome-based mayonnaise.

When compared to the laboratory-prepared samples, the commercially available mayonnaise exhibited the highest moduli values, with an initial G' of around 1550 Pa and G'' of 250 Pa. It maintained a stable LVR up to approximately 25% strain and did not reach a clear crossover point within the measured strain range, indicating the strongest solid-like behaviour. This reflects a highly stable, rigid structure that resists flow much more effectively than both the oleosome-based and control samples. In summary, all samples transitioned to more liquid-like behaviour at higher strains or stresses, allowing them to flow and spread when sufficient force was applied, a crucial characteristic for the desired texture of mayonnaise. These findings demonstrate that VCM oleosomes can effectively replace eggs in mayonnaise formulations, yielding a product with comparable viscoelastic properties, though with some textural differences compared to traditional egg-based or commercial sample. The unique rheological profile of the oleosome-based mayonnaise offers potential advantages in terms of texture and mouthfeel, making it an appealing option for consumers seeking plant-based alternatives with distinctive sensory qualities.

3.11 Sensory analysis

Physiochemical and functional property evaluation of oleosome-based mayonnaise indicates its suitability to produce emulsion-based food system. Sensory evaluation is carried out to assess the acceptability of oleosomes as a base ingredient in the formulation of eggless mayonnaise (Fig. 8). The sensory analysis of oleosome-based mayonnaise revealed superior characteristics across multiple sensory attributes compared to the traditional egg-based formulation. The visual and textural evaluation shows better characteristics in the oleosome-based formulation. Notably, appearance (8.15 ± 0.85 *vs.* 7.6 ± 0.86) and colour (8.3 ± 0.78 *vs.* 7.25 ± 0.94) scores indicated a more aesthetically pleasing product, while texture evaluation (8.0 ± 0.55 *vs.* 7.35 ± 1.11) suggested a more refined structural composition. These findings highlight the structural advantages of oleosome-based emulsions in creating visually appealing and texturally better mayonnaise alternatives. The most remarkable improvements were observed in textural attributes, with creaminess (7.85 ± 0.79 *vs.* 7.35 ± 0.73) and overall consistency (8.0 ± 0.84 *vs.* 7.75 ± 0.94) highlighting the exceptional emulsification capabilities of the oleosome base.

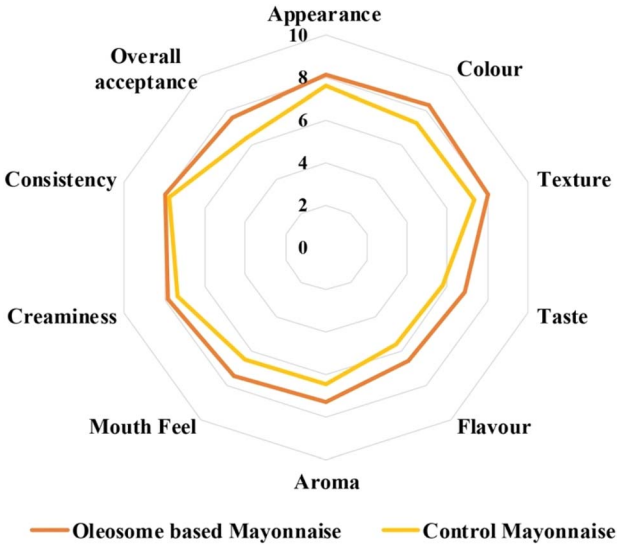

Fig. 8 Sensory profile of oleosome-based mayonnaise and control mayonnaise. Assessed on a 9-point hedonic scale (1 = dislike extremely, 9 = extremely likely).

Existing literature suggests that oleosomes demonstrate superior oxidative stability compared to bulk oils, with TAGs exhibiting a prolonged lag phase before oxidation and slower hydroperoxide formation.[72] These characteristics contribute to flavour neutrality and potentially mitigate lipid oxidation and rancidity, thereby enhancing the shelf life of the product. The mouthfeel (7.45 ± 0.97 *vs.* 6.5 ± 1.28) and aroma (7.25 ± 1.18 *vs.* 6.45 ± 1.50) score further substantiated the potential of oleosomes bringing in mouthfeel and aroma of emulsion-based foods. The overall acceptance score of 7.55 ± 0.67, which is significantly higher than the control's 6.4 ± 1.53, positions oleosome-based mayonnaise as a compelling alternative for vegan and health-conscious consumers. Taste and flavour profiles presented intriguing insights, with the oleosome-based formulation scoring 6.85 ± 1.19 and 6.6 ± 0.97, respectively, compared to the control's 5.75 ± 1.41 and 5.65 ± 1.46 while these scores suggest potential for further flavour optimisation, they nonetheless demonstrate the promising potential of oleosomes as a novel base ingredient. The superior sensory performance of the oleosome-based mayonnaise suggests its versatility as a plant-based emulsion base beyond traditional applications. While minor taste and flavour limitations were observed, these findings present promising opportunities for strategic flavour optimization in subsequent formulations. Future research should prioritize flavour profile enhancement, comprehensive stability investigations of oleosome-based emulsions, and systematic exploration of potential applications across diverse food product categories.

4 Conclusion

Virgin coconut meal (VCM), a by-product of the coconut industry, is often overlooked for its nutrition profile and either

© 2025 The Author(s). Published by the Royal Society of Chemistry

Open Access Article. Published on 30 May 2025. Downloaded on 5/21/2026 5:07:34 PM. This article is licensed under a Creative Commons Attribution-NonCommercial 3.0 Unported Licence.

used as animal feed or discarded in landfills. However, it contains a significant amount of fat (39.05 ± 1.68%), stored in the form of oleosomes, which can be effectively repurposed for food applications. This study successfully demonstrated the extraction of oleosomes from VCM for the first time and their application as a base ingredient in plant-based mayonnaise. The optimized extraction conditions were determined to be a pH of 6.43 and a feed to solvent ratio of 1 : 9.96, indicating a neutral extraction with minimal solvent pointing out the scalability of the process. Morphological analysis revealed that the oleosome core was rich in fat (93.24 ± 1.53%) and stabilised by a protein shell (5.34 ± 0.30%), making it suitable for use as the core ingredient in vegan mayonnaise production. Additionally, colour analysis and zeta potential measurements indicated a stable white coloured emulsion within the pH range of 6–8, confirming the suitability of oleosomes in emulsion-based food systems. Furthermore, sensory evaluation revealed that oleosome-based mayonnaise outperformed its egg-based counterpart in overall acceptability. Rheological analysis confirmed that oleosome-based mayonnaise exhibited a soft, solid-like texture, with enhanced spreadability and mouthfeel compared to the more rigid structure of control mayonnaise. Preliminary economic assessment revealed a significant cost reduction of 77% by using oleosomes for the production of mayonnaise compared to conventional ingredients. Cost of conventional mayonnaise was calculated to be ₹570 (approx. 7 USD), whereas, the cost of oleosome based mayonnaise was estimated to be ₹130 per kg (approx. 1.6 USD). These observations suggest the potential of oleosomes as natural emulsifiers, offering a sustainable alternative to conventional emulsifiers in food formulations. In conclusion, this study bridges the gap between waste valorization, sustainable food production, and the growing demand for plant-based alternatives. By utilizing underutilized by-products from the coconut milk industry, it presents a scalable, eco-friendly approach to developing functional food ingredients. As the food industry continues to innovate towards sustainable, plant-based products, this research provides a model for future advancements in clean-label food formulations.

Data availability

The authors confirm that all the relevant data supporting this study's findings are included in the article. Raw data files are available with the authors and can be provided upon a valid request.

Author contributions

A. A. Anoop: writing – original draft, reviewing and editing, formal analysis. P. M. Ramees: formal analysis, writing – original draft. K. V. Ragavan: conceptualization, supervision, writing– original draft, reviewing and editing.

Conflicts of interest

Authors have found no conflict of interest to declare.

Acknowledgements

Anoop thank the University Grants Commission for providing Senior Research Fellowship (NTA Ref. No.: 191620092405) to pursue doctoral work at CSIR-NIIST. Authors thank the Director of CSIR-NIIST for providing necessary infrastructure and encouragement to conduct this research work.

References

1 R. Gaillac and S. Marbach, *J. Cleaner Prod.*, 2021, **321**, 128766.
2 United Nations, The Sustainable Development Goals Report 2023: Special Edition, 2023.
3 International Coconut Community, Coconut statistics, 2021.
4 Coconut Development board, Annual report 2020–2021, 2021.
5 F. Vieira, H. E. Santana, M. Jesus, J. Santos, P. Pires, M. Vaz-Velho, D. P. Silva and D. S. Ruzene, *Sustainability*, 2024, **16**, 3066.
6 W. S. Murtius, B. D. Argo, I. Nurika and S. Sukardi, *J. Appl. Agric. Sci. Technol.*, 2024, **8**, 92–105.
7 P. Rodsamran and R. Sothornvit, *Food Chem.*, 2018, **241**, 364–371.
8 K. Karandeep, C. Navnidhi, S. Poorva, M. K. Garg and P. Anil, *Foods Raw Mater.*, 2019, **7**, 419–427.
9 A. Paucean, S. Man, S. Muste and A. Pop, *Bull. UASVM Food Sci. Technol.*, 2016, **73**, 164–166.
10 S. Hossain, M. R. I. Shishir, M. Saifullah, M. S. Kayshar, S. W. Tonmoy, A. Rahman and M. Shams-Ud-Din, *Int. J. Nutr. Food Sci.*, 2016, **5**, 31–38.
11 K. Gunathilake and Y. Abeyrathne, *J. Food Process. Preserv.*, 2008, **32**, 133–142.
12 R. Zolqadri, Z. Akbarbaglu, K. Sarabandi, S. H. Peighambardoust, S. M. Jafari and A. M. Khaneghah, *Food Funct.*, 2024, **15**, 11266–11279.
13 A. Naik, S. Raghavendra and K. Raghavarao, *Appl. Biochem. Biotechnol.*, 2012, **167**, 1290–1302.
14 J. Weiss and H. Zhang, *Trends Food Sci. Technol.*, 2020, **106**, 322–332.
15 J. Ding, J. Wen, J. Wang, R. Tian, L. Yu, L. Jiang, Y. Zhang and X. Sui, *Food Hydrocolloids*, 2020, **100**, 105418.
16 F. Bramante, V. di Bari, G. Adams, F. Beaudoin, G. Waschatko, R. Jakobi, N. Billecke and D. Gray, *J. Food Eng.*, 2025, 112471.
17 D. Karefyllakis, A. J. Van Der Goot and C. V. Nikiforidis, *Soft Matter*, 2019, **15**, 4639–4646.
18 Y. Peng, Z. Shan, W. Jia, M. Li, X. Wen and Y. Ni, *J. Food Eng.*, 2025, **386**, 112292.
19 M. J. Romero-Guzman, E. Vardaka, R. M. Boom and C. V. Nikiforidis, *Food Bioprod. Process.*, 2020, **121**, 230–237.
20 G. Waschatko, A. Junghans and T. A. Vilgis, *Faraday Discuss.*, 2012, **158**, 157–169.
21 K. Ayan, R. M. Boom and C. V. Nikiforidis, *J. Food Eng.*, 2024, **381**, 112188.
22 C. Qin, R. Fu, Y. Mei, X. Wen, Y. Ni, R. M. Boom and C. V. Nikiforidis, *J. Food Eng.*, 2024, **368**, 111908.

© 2025 The Author(s). Published by the Royal Society of Chemistry

Open Access Article. Published on 30 May 2025. Downloaded on 5/21/2026 5:07:34 PM. This article is licensed under a Creative Commons Attribution-NonCommercial 3.0 Unported Licence.

23 M. J. Romero-Guzman, L. Jung, K. Kyriakopoulou, R. M. Boom and C. V. Nikiforidis, *J. Food Eng.*, 2020, **276**, 109890.
24 T. Fujii, *Biosci., Biotechnol., Biochem.*, 2017, **81**, 680–686.
25 S. Gallier, K. C. Gordon and H. Singh, *Food Chem.*, 2012, **132**, 1996–2006.
26 S. M. Ghazani, J. Hargreaves, B. Guldiken, A. Mata, E. Pensini and A. G. Marangoni, *Curr. Res. Food Sci.*, 2024, **8**, 100682.
27 A. Matsakidou, C. G. Biliaderis and V. Kiosseoglou, *Food Hydrocolloids*, 2013, **30**, 232–240.
28 C. V. Nikiforidis, A. Matsakidou and V. Kiosseoglou, *RSC Adv.*, 2014, **4**, 25067–25078.
29 G. E. Box and D. W. Behnken, *Technometrics*, 1960, **2**, 455–475.
30 Association of Official Analytical Chemists, Official methods of analysis of the Association of Official Analytical Chemists, The Association, 2000, vol. **11**.
31 S. Worrasinchai, M. Suphantharika, S. Pinjai and P. Jamnong, *Food Hydrocolloids*, 2006, **20**, 68–78.
32 S. Xia, S. Shen, J. Song, K. Li, X. Qin, X. Jiang, C. Xue and Y. Xue, *Food Chem.*, 2023, **402**, 134265.
33 J. Ding, Z. Xu, B. Qi, Z. Liu, L. Yu, Z. Yan, L. Jiang and X. Sui, *Int. J. Food Sci. Technol.*, 2020, **55**, 229–238.
34 L.-J. Lin, P.-C. Liao, H.-H. Yang and J. T. C. Tzen, *Plant Physiol. Biochem.*, 2005, **43**, 770–776.
35 D. A. Gray, G. Payne, D. J. McClements, E. A. Decker and M. Lad, *Eur. J. Lipid Sci. Technol.*, 2010, **112**, 741–749.
36 S. D. Chirico, V. di Bari, T. Foster and D. Gray, *Food Chem.*, 2018, **241**, 419–426.
37 M. J. Romero-Guzmán, N. Köllmann, L. Zhang, R. M. Boom and C. V. Nikiforidis, *LWT*, 2020, **123**, 109120.
38 M. J. Romero-Guzman, N. Kollmann, L. Zhang, R. M. Boom and C. V. Nikiforidis, *LWT*, 2020, **123**, 109120.
39 U. S. Vardar, J. H. Bitter and C. V. Nikiforidis, *Colloids Surf., B*, 2024, **236**, 113819.
40 J. Yang, U. S. Vardar, R. M. Boom, J. H. Bitter and C. V. Nikiforidis, *Food Hydrocolloids*, 2023, **145**, 109078.
41 Y. Ying, L. Zhao, L. Kong, X. Kong, Y. Hua and Y. Chen, *Food Chem.*, 2015, **181**, 179–185.
42 M. Kaszuba, J. Corbett, F. M. Watson and A. Jones, *Philos. Trans. R. Soc., A*, 2010, **368**, 4439–4451.
43 Y. Wang, D. Li, L.-J. Wang and B. Adhikari, *J. Food Eng.*, 2011, **104**, 56–62.
44 G. I. Frandsen, J. Mundy and J. T. Tzen, *Physiol. Plant.*, 2001, **112**, 301–307.
45 B. Qi, J. Ding, Z. Wang, Y. Li, C. Ma, F. Chen, X. Sui and L. Jiang, *Food Res. Int.*, 2017, **100**, 551–557.
46 Y. Cao, L. Zhao, Y. Ying, X. Kong, Y. Hua and Y. Chen, *Food Chem.*, 2015, **177**, 288–294.
47 X. Chen, L. Zhang, L. Zhang, W. Sun, Z. Zhang, H. Liu, Y. Bu and R. I. Cukier, *J. Phys. Chem. Lett.*, 2010, **1**, 1637–1641.
48 A. Rohman, Y. B. Che Man, A. Ismail and P. Hashim, *J. Am. Oil Chem. Soc.*, 2010, **87**, 601–606.
49 N. Vlachos, Y. Skopelitis, M. Psaroudaki, V. Konstantinidou, A. Chatzilazarou and E. Tegou, *Anal. Chim. Acta*, 2006, **573**, 459–465.
50 A. Rohman, *Int. J. Food Prop.*, 2017, **20**, 1447–1456.
51 R. Gunarathne, N. Marikkar, E. Mendis, C. Yalegama, L. Jayasinghe and S. Ulpathakumbura, *J. Food Chem. Nanotechnol.*, 2022, **8**(3), 69–75.
52 P. T. Aliman, R. F. N. Cada, M. K. P. Devanadera, A. M. Labrador and M. R. Santiago-Bautista, *Acta Med. Philipp.*, 2021, **55**(4).
53 R. Gunarathne, N. Marikkar, E. Mendis, C. Yalegama, L. Jayasinghe and S. Ulpathakumbura, *J. Food Chem. Nanotechnol.*, 2022, **8**, 69–75.
54 L. Yuzhen, D. Changwen, S. Yanqiu and Z. Jianmin, *J. Food Sci. Eng.*, 2014, **4**, 244–249.
55 K. Kwon, K. H. Park and K. C. Rhee, *J. Agric. Food Chem.*, 1996, **44**, 1741–1745.
56 R. M. Amir, F. M. Anjum, M. I. Khan, M. R. Khan, I. Pasha and M. Nadeem, *J. Food Sci. Technol.*, 2013, **50**, 1018–1023.
57 S. Dıblan, P. Kadiroglu and L. Y. Aydemir, *Food Health*, 2018, **4**, 80–88.
58 J. Kong and S. Yu, *Acta Biochim. Biophys. Sin*, 2007, **39**, 549–559.
59 N. Li, G. Qi, X. S. Sun, D. Wang, S. Bean and D. Blackwell, *Trans. ASABE*, 2014, **57**, 169–178.
60 M. Ibrahim, M. Alaam, H. El-Haes, A. F. Jalbout and A. de Leon, *Ecletica Quim.*, 2006, **31**, 15–21.
61 S. Chumwaengwapee, S. Soontornchai and K. Thongprajukaew, *ScienceAsia*, 2013, **39**, 636–642.
62 R. Nandasiri, B. Silva, N. Senevirathene, H. Munasinghe, S. De Silva and R. Jayatissa, *Comparison of the fatty acid composition of different culinary oils with high-saturated coconut oil towards the improvement of public health*, Wiley 111, River ST, Hoboken 07030-5774, NJ USA, 2022, vol. 99, p. 120.
63 Y. Srivastava, A. D. Semwal, V. A. Sajeevkumar and G. Sharma, *J. Food Sci. Technol.*, 2017, **54**, 45–54.
64 X. Duan, Z. Yu, L. Zhou, D. He, X. Jiang and F. Lei, *LWT*, 2025, 117554.
65 V. U. Celenk, Z. P. Gumus and Z. Ustun Argon, in *Bioactive Phytochemicals from Vegetable Oil and Oilseed Processing By-Products*, Springer, 2023, pp. 309–321.
66 B. J. Villarino, L. M. Dy and M. C. C. Lizada, *LWT*, 2007, **40**, 193–199.
67 A. Kovalcuks, E. Straumite and M. Duma, *Rural Sustainability Res.*, 2016, **35**, 24–31.
68 M. Havaux, *Plant J.*, 2014, **79**, 597–606.
69 D. J. McClements, *Food Emulsions: Principles, Practices, and Techniques*, CRC press, 2004.
70 S. E. Quintana, M. Zuñiga-Navarro, D. Ramirez-Brewer and L. A. García-Zapateiro, *Fluids*, 2023, **8**, 287.
71 A. Tamas, S. Nitu, S. Popa and M. Padure, *Chem. J. Mold.*, 2023, **18**, 52–60.
72 L. Plankensteiner, C. V. Nikiforidis, J. Vincken and M. Hennebelle, *J. Am. Oil Chem. Soc.*, 2025, **102**(2), 435–449.

© 2025 The Author(s). Published by the Royal Society of Chemistry